

# SARS-CoV-2 B.1.1.7 escape from mRNA vaccine-elicited neutralizing antibodies

**Ravindra Gupta** (✉ [rkg20@cam.ac.uk](mailto:rkg20@cam.ac.uk))

University of Cambridge <https://orcid.org/0000-0001-9751-1808>

**Dami Collier**

University College London <https://orcid.org/0000-0001-5446-4423>

**Anna De Marco**

Humabs BioMed SA, a subsidiary of Vir Biotechnology, Inc

**Isabella Ferreira**

Cambridge University

**Bo Meng**

University of Cambridge

**Rawlings Datir**

University of Cambridge

**Alexandra Walls**

University of Washington

**Steven Kemp**

University College London

**Jessica Bassi**

Vir Biotechnology

**Dora Pinto**

Humabs BioMed SA, a subsidiary of Vir Biotechnology, Inc

**Chiara Silacci-Fregni**

Institute for Research in Biomedicine, Università della Svizzera italiana

**Siro Bianchi**

Vir Biotechnology <https://orcid.org/0000-0002-5100-8905>

**M. Alejandra Tortorici**

University of Washington <https://orcid.org/0000-0002-2260-2577>

**John Bowen**

University of Washington

**Katja Culap**

Humabs BioMed SA, a subsidiary of Vir Biotechnology, Inc <https://orcid.org/0000-0002-0956-0018>

**Stefano Jaconi**

Humabs BioMed SA, a subsidiary of Vir Biotechnology, Inc

**Elisabetta Cameroni**

Humabs BioMed SA, a subsidiary of Vir Biotechnology, Inc

**Gyorgy Snell**

Vir Biotechnology

**Matteo Pizzuto**

Vir Biotechnology, Inc

**Alessandra Pallanda**

Clinica Luganese Moncucco

**Christian Gorzoni**

Clinica Luganese Moncucco

**Agostino Riva**

University of Milan

**Anne Elmer**

NIHR Cambridge Clinical Research Facility

**The CITIID-NIHR BioResource COVID-19 Collaboration**

COVID-19 Collaboration

**Barbara Graves**

NIHR Cambridge Clinical Research Facility

**Laura McCoy**

University College London <https://orcid.org/0000-0001-9503-7946>

**Ken Smith**

University of Cambridge

**John Bradley**

University of Cambridge

**James Thaventhiran**

MRC Toxicology Unit <https://orcid.org/0000-0001-8616-074X>

**Lourdes Ceron-Gutierrez1**

Addenbrookes Hospital

**Gabriela Barcenas-Morales**

UNAM

**Herbert Virgin**

Vir Biotechnology, Washington University School of Medicine <https://orcid.org/0000-0001-8580-7628>

**Antonio Lanzavecchia**

Università della Svizzera italiana <https://orcid.org/0000-0002-3041-7240>

**Luca Piccoli**

Institute for Research in Biomedicine, Università della Svizzera italiana, Bellinzona

<https://orcid.org/0000-0002-1085-6502>

**Rainer Doffinger**

Addenbrooke's Hospital <https://orcid.org/0000-0002-9841-3617>

**Mark Wills**

Cambridge University

**David Veesler**

University of Washington <https://orcid.org/0000-0002-6019-8675>

**Davide Corti**

Vir Biotechnology <https://orcid.org/0000-0002-5797-1364>

---

## Biological Sciences - Article

**Keywords:** SARS-CoV-2, COVID-19, antibody, vaccine, neutralising antibodies, 36 mutation

**Posted Date:** January 29th, 2021

**DOI:** <https://doi.org/10.21203/rs.3.rs-156101/v1>

**License:**  This work is licensed under a Creative Commons Attribution 4.0 International License.

[Read Full License](#)

---

**Version of Record:** A version of this preprint was published at Nature on March 11th, 2021. See the published version at <https://doi.org/10.1038/s41586-021-03412-7>.

1 **SARS-CoV-2 B.1.1.7 escape from mRNA vaccine-elicited neutralizing antibodies**

2  
3 Dami A. Collier<sup>1,2,3\*</sup>, Anna De Marco<sup>4\*</sup>, Isabella A.T.M. Ferreira<sup>\*1,2</sup>, Bo Meng<sup>1,2\*</sup>, Rawlings  
4 Datir <sup>\*1,2,3</sup>, Alexandra C. Walls<sup>5</sup>, Steven A. Kemp S<sup>1,2,3</sup>, Jessica Bassi<sup>4</sup>, Dora Pinto<sup>4</sup>, Chiara  
5 Silacci Fregni<sup>4</sup>, Siro Bianchi<sup>4</sup>, M. Alejandra Tortorici<sup>5</sup>, John Bowen<sup>5</sup>, Katja Culap<sup>4</sup>, Stefano  
6 Jaconi<sup>4</sup>, Elisabetta Cameroni<sup>4</sup>, Gyorgy Snell<sup>6</sup>, Matteo S. Pizzuto<sup>4</sup>, Alessandra Franzetti  
7 Pellanda<sup>7</sup>, Christian Garzoni<sup>7</sup>, Agostino Riva<sup>8</sup>, The CITIID-NIHR BioResource COVID-19  
8 Collaboration<sup>9</sup>, Anne Elmer<sup>10</sup>, Nathalie Kingston<sup>10</sup>, Barbara Graves <sup>10</sup>, Laura E McCoy<sup>3</sup>,  
9 Kenneth GC Smith <sup>1,2</sup>, John R. Bradley <sup>2,10</sup>, James Thaventhiran J<sup>2</sup>, Lourdes Ceron-  
10 Gutierrez L<sup>11</sup>, Gabriela Barcenas-Morales <sup>11,12</sup>, Herbert W. Virgin<sup>6</sup>, Antonio Lanzavecchia<sup>4</sup>,  
11 Luca Piccoli<sup>4</sup>, Rainer Doffinger<sup>11</sup>, Mark Wills<sup>2</sup>, David Veessler<sup>5</sup>, Davide Corti<sup>4\*</sup>, Ravindra K.  
12 Gupta<sup>1,2, 13\*</sup>

13  
14 \*Equal contribution

15  
16 <sup>1</sup>Cambridge Institute of Therapeutic Immunology & Infectious Disease (CITIID), Cambridge, UK.

17 <sup>2</sup>Department of Medicine, University of Cambridge, Cambridge, UK.

18 <sup>3</sup>Division of Infection and Immunity, University College London, London, UK.

19 <sup>4</sup>Humabs Biomed SA, a subsidiary of Vir Biotechnology, 6500 Bellinzona, Switzerland.

20 <sup>5</sup>Department of Biochemistry, University of Washington, Seattle, WA 98195, USA

21 <sup>6</sup>Vir Biotechnology, San Francisco, CA 94158, USA.

22 <sup>7</sup>Clinic of Internal Medicine and Infectious Diseases, Clinica Luganese Moncucco, 6900 Lugano,  
23 Switzerland

24 <sup>8</sup>Division of Infectious Diseases, ASST Fatebenefratelli Sacco, Luigi Sacco Hospital, University of  
25 Milan, 20157 Milan, Italy

26 <sup>9</sup>The CITIID-NIHR BioResource COVID-19 Collaboration, see appendix 1 for author list

27 <sup>10</sup>NIHR Cambridge Clinical Research Facility, Cambridge, UK.

28 <sup>11</sup>Department of Clinical Biochemistry and Immunology, Addenbrookes Hospital, UK

29 <sup>12</sup>Laboratorio de Inmunologia, S-Cuautitlán, UNAM, Mexico

30 <sup>13</sup>Africa Health Research Institute, Durban, South Africa

31  
32  
33 **Correspondence:** [dcorti@vir.bio](mailto:dcorti@vir.bio), [rkg20@cam.ac.uk](mailto:rkg20@cam.ac.uk)

34  
35 **Key words:** SARS-CoV-2; COVID-19; antibody, vaccine, neutralising antibodies;  
36 **mutation;**

37

## 38 Abstract

39 SARS-CoV-2 transmission is uncontrolled in many parts of the world, compounded in  
40 some areas by higher transmission potential of the B.1.1.7 variant now seen in 50 countries.  
41 It is unclear whether responses to SARS-CoV-2 vaccines based on the prototypic strain  
42 will be impacted by mutations found in B.1.1.7. Here we assessed immune responses  
43 following vaccination with mRNA-based vaccine BNT162b2. We measured neutralising  
44 antibody responses following a single immunization using pseudoviruses expressing the  
45 wild-type Spike protein or the 8 mutations found in the B.1.1.7 Spike protein. The vaccine  
46 sera exhibited a broad range of neutralizing titres against the wild-type pseudoviruses  
47 (<1:4 to 3449) that were reduced against B.1.1.7 variant by 3.85 fold (IQR 2.68-5.28). This  
48 reduction was also evident in sera from some convalescent patients. Decreased B.1.1.7  
49 neutralization was also observed with monoclonal antibodies targeting the N-terminal  
50 domain (9 out of 10), the Receptor Binding Motif (RBM) (5 out of 29), but not in  
51 neutralizing mAbs binding outside the RBM. Introduction of the E484K mutation in a  
52 B.1.1.7 background led to a further loss of neutralizing activity by vaccine-elicited  
53 antibodies over that conferred by the B.1.1.7 mutations alone. Further work is needed to  
54 establish the impact of these observations on protective vaccine efficacy in the context of  
55 the evolving B.1.1.7 lineage that will likely acquire E484K.

## 57 Introduction

58 The outbreak of a pneumonia of unknown cause in Wuhan, China in December 2019,  
59 culminated in a global pandemic due to a novel viral pathogen, now known to be SARS-COV-  
60 2<sup>1</sup>. The unprecedented scientific response to this global challenge has led to the rapid  
61 development of vaccines aimed at preventing SARS-COV-2 infection and transmission.  
62 Continued viral evolution led to the emergence and selection of SARS-CoV-2 variants with  
63 enhanced infectivity/transmissibility<sup>2,3 4,5</sup> and ability to circumvent drug<sup>6</sup> and immune  
64 control<sup>7,8</sup>.

65 SARS-CoV-2 vaccines have recently been licensed that target the Spike (S) protein,  
66 either using mRNA or adenovirus vector technology with protection rates over a few months  
67 ranging from 62 to 95%<sup>9-11</sup>. The BNT162b2 vaccine encodes the full-length trimerised S protein  
68 of SARS CoV-2 and is formulated in lipid nanoparticles to optimise delivery to cells<sup>12</sup>. Other  
69 vaccines include the Moderna mRNA-1273 vaccine, which is also a lipid nanoparticle  
70 formulated S glycoprotein<sup>13</sup> and the Oxford-AstraZeneca ChAdOx1 nCoV-19 vaccine  
71 (AZD1222) which is a replication-deficient chimpanzee adenoviral vector ChAdOx1,  
72 containing the S glycoprotein<sup>14</sup>. The duration of immunity conferred by these vaccines is as yet  
73 unknown. These vaccines were designed against the Wuhan-1 isolate discovered in 2019.  
74 Concerns have been raised as to whether these vaccines will be effective against new SARS-  
75 CoV-2 variants, such as B.1.1.7 (N501Y.V1), B.1.351 (N501Y.V2) and P1 (N501Y.V2) that

76 originated in the UK, South Africa, and Brazil and are now being detected all over the world<sup>15-</sup>  
77 <sup>17</sup>.

78 The phase I/II studies of the Pfizer-BioNTech BNT162b2 vaccine determined the  
79 immunogenicity of different dosing regimens. The geometric mean concentration (GMC) of  
80 RBD-binding IgG 21 days after the first dose of 30 µg of the BNT162b2 vaccine, which is the  
81 dose approved in the UK, was higher than the GMC of a panel of convalescent plasma (1,536  
82 vs 602 U/ml). Nevertheless, the corresponding neutralisation geometric mean titre (GMT) was  
83 3-fold lower than a panel of convalescent plasma (29 vs 94)<sup>12</sup>, but substantially increased after  
84 boost immunization<sup>18</sup>. In older adults mean GMT was only 12 in a preliminary analysis of 12  
85 participants<sup>19</sup> and increased to 109 after the second dose.

86 In this study, we assess antibody responses induced three weeks after vaccination with  
87 the first dose of BNT162b2 following the rollout in the UK. In addition, by using a panel of  
88 human neutralizing monoclonal antibodies (mAbs) we show that the B.1.1.7 variant can escape  
89 neutralization mediated by most NTD-specific antibodies tested and by a fraction of RBM-  
90 specific antibodies. We also show that the recent appearance of the E484K mutation in B.1.1.7  
91 isolates from the UK, similarly to the B.1.351 and P1 isolates, results in incremental loss of  
92 neutralization by BNT162b2 mRNA-elicited antibodies.

93

## 94 **Results**

95 Twenty-three participants had received the BNT162b2 mRNA vaccine three weeks prior to  
96 blood draw for serum and peripheral blood mononuclear cells (PBMC) collection. Median age  
97 was 82 years (IQR 64-85) and 30% were female (**Table 1**). Serum IgG titres to N protein, S  
98 and the S RBD were assayed by particle based flow cytometry on a Luminex analyser (**Fig. 1a**).  
99 These data showed Spike and RBD antibody titres much higher than in healthy controls, similar  
100 to both convalescent plasma units used for therapeutic purposes as well as to serum from  
101 recovered individuals. The raised N titres relative to control could be the result of non specific  
102 cross reactivity that is increased following vaccination. However, the antibody response was  
103 heterogeneous with almost 100-fold variation in IgG titres to S and Spike RBD across the  
104 vaccinated participants.

105 Using lentiviral pseudotyping we generated wild type S proteins on the surface of enveloped  
106 virions in order to measure neutralisation activity of vaccine-elicited sera. This system has been  
107 shown to give results correlating with replication competent authentic virus<sup>20,21</sup>. The vaccine

108 sera exhibited a range of inhibitory dilutions giving 50% neutralisation (ID<sub>50</sub>) ≤4 to 3449 (**Fig.**  
109 **1c-d**). The GMT against wild type (WT) pseudovirus was 24. Eight out of 23 participants  
110 exhibited no appreciable neutralisation against the WT pseudotyped virus. There was  
111 reasonable correlation between full length S IgG titres and serum neutralisation titres  
112 (**Extended Data Fig. 1a**). A broad range of T cell responses was measured by IFN gamma  
113 FLUOROSPOT against SARS-CoV-2 peptides in vaccinees. These cell responses did not  
114 correlate with IgG S antibody titres, but there was some correlation with serum neutralisation  
115 against WT virus (**Extended Data Fig. 1b-c**).

116 We next generated mutated pseudoviruses carrying S protein with mutations N501Y,  
117 A570D and the H69/V70 deletion. We observed no reduction in the ability of sera from  
118 vaccinees to inhibit either WT or mutant virus (**Extended Data Fig. 2**). In fact, we observed  
119 that vaccine sera displayed higher neutralizing activity against the N501Y, A570D and  
120 H69/V70 deletion mutant relative to WT virus. Next, we then tested a panel of sera from 11  
121 recovered individuals and found that these sera also neutralised both wild type and the mutated  
122 viruses similarly (**Extended Data Fig. 3**). The findings for vaccine sera may be related to a  
123 potential allosteric effect of ΔH69/V70 that might enhance neutralization by antibodies  
124 targeting cryptic sites on the S, such as the RBD site II (also named as class 4 site).

125 We then generated the full set of eight mutations in the S protein present in B.1.1.7  
126 variant (**Fig. 1b** and **Table 1**), ΔH69/V70, Δ144, N501Y and A570D in the S<sub>1</sub> subunit and  
127 P681H, T716I, S982A and D1118H in the S<sub>2</sub> subunit. All constructs also contained D614G. We  
128 found that among 15 individuals with neutralisation activity three weeks after receiving a single  
129 dose of the the BNT162b2 mRNA vaccine, 10 showed evidence of reduction in efficacy of  
130 antibodies against the B.1.1.7 mutant (fold change >3) (**Fig. 1c-d**). The highest fold change was  
131 approximately 6 and the median fold change was 3.85 (IQR 2.68-5.28). Amongst sera from 7  
132 recovered individuals, only 2 demonstrated reduced potency against B.1.1.7 (**Fig. 1e-h** and  
133 **Extended Data Fig. 4**).

#### 134 **B.1.1.7 variant escapes from NTD- and RBM-specific mAb-mediated neutralization.**

135 To investigate the role of the full set of mutations in NTD, RBD and S2 present in the B.1.1.7  
136 variant, we tested 61 mAbs isolated from 15 individuals that recovered from WT SARS-CoV-  
137 2 infection with an *in-vitro* pseudotyped neutralization assay using VeroE6 target cells  
138 expressing TMPRSS2 (**Extended Data Table 1**). We found that 20 out of 61 (32.8%) mAbs

139 showed a greater than 2-fold loss of neutralizing activity of B.1.1.7 variant compared to WT  
140 SARS-CoV-2 (**Fig. 2a,b** and **Extended Data Fig. 5**). Remarkably, the B.1.1.7 mutant virus  
141 was found to fully escape neutralization by 7 out of 10 NTD-targeting mAbs (70%), and partial  
142 escape from additional 2 mAbs (20%) (**Fig. 2c**). We previously showed that the deletion of  
143 residue 144 abrogates binding by 4 out of 6 NTD-specific mAbs tested, possibly accounting  
144 for viral neutralization escape by most NTD-specific antibodies<sup>22</sup>. Of the 29 RBM-targeting  
145 mAbs, 5 (17.2%) showed more than 100-fold decrease in B.1.1.7 neutralization, and additional  
146 6 mAbs (20.7%) had a partial 2-to-10-fold reduction (**Fig. 2d**). Finally, all RBD-specific non-  
147 RBM-targeting mAbs tested fully retained B.1.1.7 neutralizing activity (**Fig. 2e**).

148 To address the role of B.1.1.7 N501Y mutation in the neutralization escape from RBM-  
149 specific antibodies, we tested the binding of 51 RBD-specific mAbs to WT and N501Y mutant  
150 RBD by biolayer interferometry (**Fig. 2f** and **Extended Data Fig. 6**). The 5 RBM-specific  
151 mAbs that failed to neutralize B.1.1.7 variant (**Fig. 2d**) showed a complete loss of binding to  
152 N501Y RBD mutant (**Fig. 2g, h**), demonstrating a critical role for this mutation as an escape  
153 mechanism for RBM-targeting mAbs.

154 The decreased neutralizing activity of the immune sera from vaccinees and  
155 convalescent patients against B.1.1.7, but not against  $\Delta 69/70$ -501Y-570D mutant (**Fig. 1** and  
156 **Extended Data Fig. 2**), could be the result of a loss of neutralizing activity of both RBD- and  
157 NTD-targeting antibodies, and suggests that the key mutations driving polyclonal escape are  
158  $\Delta 144$  and N501Y.

159

## 160 SARS-CoV-2 B.1.1.7 binds human ACE2 with higher affinity than WT

161 SARS-CoV-2 and SARS-CoV enter host cells through binding of the S glycoprotein to  
162 ACE2<sup>1,23</sup>. Previous studies showed that the binding affinity of SARS-CoV for human ACE2  
163 correlated with the rate of viral replication in distinct species, transmissibility and disease  
164 severity<sup>24-26</sup>. To understand the potential contribution of receptor interaction to infectivity, we  
165 set out to evaluate the influence of the B.1.1.7 RBD substitution N501Y on receptor  
166 engagement. We used biolayer interferometry to study binding kinetics and affinity of the  
167 purified human ACE2 ectodomain (residues 1-615) to immobilized biotinylated SARS-CoV-2  
168 B.1.1.7 or WT RBDs. We found that ACE2 bound to the B.1.1.7 RBD with an affinity of 22  
169 nM compared to 133 nM for the WT RBD (**Extended Data Fig. 7**), in agreement with our  
170 previous deep-mutational scanning measurements using dimeric ACE2<sup>27</sup>. Although ACE2  
171 bound with comparable on-rates to both RBDs, the observed dissociation rate constant was  
172 slower for B.1.1.7 than for the WT RBD (**Table 2**). Enhanced binding of the B.1.1.7 RBD to



173 human ACE2 resulting from the N501Y mutation might participate to the efficient ongoing  
174 transmission of this newly emerged SARS-CoV-2 lineage, and possibly reduced opportunity  
175 for antibody binding.

176

177 **Further loss of neutralization of vaccine-elicited antibodies against a B.1.1.7 Spike**  
178 **carrying E484K mutation**

179 E484K as a lone Spike mutation is present in the UK ([https://www.cogconsortium.uk/wp-](https://www.cogconsortium.uk/wp-content/uploads/2021/01/Report-2_COG-UK_SARS-CoV-2-Mutations.pdf)  
180 [content/uploads/2021/01/Report-2\\_COG-UK\\_SARS-CoV-2-Mutations.pdf](https://www.cogconsortium.uk/wp-content/uploads/2021/01/Report-2_COG-UK_SARS-CoV-2-Mutations.pdf)). Given the  
181 inevitability of E484K emerging on the background of B.1.1.7, we generated data on the  
182 potency of vaccine sera against this combination. When testing B.1.1.7 with E484K against  
183 vaccine sera from five individuals, we observed a significant additional loss of neutralising  
184 activity (**Fig. 3**).

## 185 Discussion

186 Serum neutralizing activity is a correlate of protection for other respiratory viruses, including  
187 influenza<sup>28</sup> and respiratory syncytial virus where prophylaxis with monoclonal antibodies has  
188 been used in at-risk groups<sup>29,30</sup>. Neutralising antibody titres appeared to be highly correlated  
189 with vaccine protection against SARS-CoV-2 rechallenge in non-human primates, and  
190 importantly, there was no correlation between T cell responses (as measured by ELISPOT) and  
191 protection<sup>31</sup>. Moreover, passive transfer of purified polyclonal IgGs from convalescent  
192 macaques protected naïve macaques against subsequent SARS-CoV-2 challenge<sup>32</sup>. Coupled  
193 with multiple reports of re-infection, there has therefore been significant attention placed on  
194 virus neutralisation.

195 This is the first study reporting on the neutralisation escape from sera collected after one  
196 dose of the BNT162b2 vaccine in individuals. The participants of this study had a median age  
197 of over 80, in line with the targeting of this age group in the initial rollout of the vaccination  
198 campaign in the UK. Participants showed similar neutralising activity against wild type  
199 pseudovirus as in the phase I/II study, with geometric mean titres of 24 and 29, respectively<sup>12</sup>.  
200 The three mutations in S (N501Y, A570D,  $\Delta$ H69/V70) did not appear to impact neutralisation  
201 in a pseudovirus assay. However, we demonstrated that a pseudovirus bearing S protein with  
202 the full set of mutations present in the B.1.1.7 variant (i.e.,  $\Delta$ H69/V70,  $\Delta$ I144, N501Y, A570D,  
203 P681H, T716I, S982A, D1118H) did result in reduced neutralisation by sera from vaccinees. A  
204 reduction in neutralization titres from mRNA-elicited antibodies in volunteers who received  
205 two doses (using both mRNA-1273 and BNT162b2 vaccines) was also observed by Wang et  
206 al.<sup>33</sup> using pseudoviruses carrying the N501Y mutation. Another study reported on a modest  
207 and not significant (average 1.2 fold) reduction of neutralization against the B.1.1.7 variant in  
208 sera from individuals vaccinated with two doses of mRNA-1273<sup>34</sup>. The level of neutralizing  
209 antibodies observed in both of these studies was approximately one log higher than the one  
210 observed in the cohort of vaccinees described in this study. This may be related to the older age  
211 of the individuals from this study as well as to the fact that these were exposed to only one dose  
212 of the BNT162b2 vaccine. In general, it is expected that the effect of mutations on the  
213 neutralization by polyclonal serum antibodies might be more prominent on low-titre in contrast  
214 to high-titre sera. It is important to study virus neutralisation at lower serum neutralisation titres  
215 because decline in neutralisation titres over time is expected to occur following vaccination.

216 The reduced neutralizing activity observed with polyclonal antibodies elicited by  
217 mRNA vaccines observed in this study and in Wang et al.<sup>33</sup> is further supported by the loss of  
218 neutralizing activity observed with human mAbs directed to both RBD and, to a major extent,  
219 to NTD. In the study by Wang et al., 6 out of 17 RDB-specific mAbs isolated from mRNA-1273  
220 vaccinated individuals showed more than 100-fold neutralization loss against N501Y mutant,  
221 a finding that is consistent with the loss of neutralization by 5 out of 29 RBM-specific mAbs  
222 described in this study.

223 Multiple variants, including the 501Y.V2 and B.1.1.7 lineages, harbor multiple  
224 mutations as well as deletions in NTD, most of which are located in a site of vulnerability that  
225 is targeted by all known NTD-specific neutralizing antibodies<sup>22</sup>. The role of NTD-specific  
226 neutralizing antibodies might be under-estimated, in part by the use of neutralization assays  
227 based on target cells over-expressing ACE2 receptor. NTD-specific mAbs were suggested to  
228 interfere with viral entry based on other accessory receptors, such as DC-SIGN and L-SIGN<sup>35</sup>,  
229 and their neutralization potency was found to be dependent on different in vitro culture  
230 conditions<sup>22</sup>. The observation that 9 out of 10 NTD-specific neutralizing antibodies failed to  
231 show a complete or near-complete loss of neutralizing activity against B.1.1.7 indicates that  
232 this new variant may have evolved also to escape from this class of antibodies, that may have  
233 a yet unrecognized role in protective immunity. Wibmer et al.<sup>36</sup> have also recently reported the  
234 loss of neutralization of 501Y.V2 by the NTD-specific mAb 4A8, likely driven by the R246I  
235 mutation. This result is in line with the lack of neutralization of B.1.1.7 by 4A8 mAb observed  
236 in this study, likely caused by  $\Delta$ 144 due to loss of binding<sup>22</sup>. Finally, the role of NTD mutations  
237 (in particular, L18F,  $\Delta$ 242-244 and R246I) was further supported by the marked loss of  
238 neutralization observed by Wibmer et al.<sup>36</sup> against 501Y.V2 compared to the chimeric virus  
239 carrying only the RBD mutations K417N, E484K and N501Y. Taken together, the presence of  
240 multiple escape mutations in NTD is supportive of the hypothesis that this region of the Spike,  
241 in addition to RBM, is also under immune pressure.

242 E484K as a lone Spike mutation is present in the UK  
243 ([https://www.cogconsortium.uk/wp-content/uploads/2021/01/Report-2\\_COG-UK\\_SARS-](https://www.cogconsortium.uk/wp-content/uploads/2021/01/Report-2_COG-UK_SARS-CoV-2-Mutations.pdf)  
244 [CoV-2-Mutations.pdf](https://www.cogconsortium.uk/wp-content/uploads/2021/01/Report-2_COG-UK_SARS-CoV-2-Mutations.pdf)). It is inevitable that E484K will emerge in the background of B.1.1.7  
245 and we therefore generated data on the potency of vaccine sera against this combination. E484K  
246 has been shown to impact neutralisation by monoclonal antibodies or convalescent sera,  
247 especially in combination with N501Y and K417N<sup>16,37-39</sup>. Here we show further reduction

248 neutralisation titers by vaccine sera when E484K is present alongside the B.1.1.7 S mutations.  
249 Consistent with our findings, Wu and co-authors<sup>34</sup> have shown that variants carrying the E484K  
250 mutation resulted in 3-to-6 fold reduction in neutralization by sera from mRNA-1273  
251 vaccinated individuals.

252 Our study was limited by relatively small sample size. Although the Spike pseudotyping system  
253 has been shown to faithfully represent full length infectious virus, there may be determinants  
254 outside the S that influence escape from antibody neutralization either directly or indirectly in  
255 a live replication competent system. On the other hand live virus systems allow replication and  
256 therefore mutation to occur, and rigorous sequencing at multiple steps is needed.

257 Amidst high transmission in many parts of the world, vaccines are a key part of a long term  
258 strategy to bring SARS-CoV-2 under control. Our data suggest that vaccine escape will be  
259 inevitable in the future, and should be mitigated by designing next generation vaccines with  
260 mutated S sequences and using alternative viral antigens. Currently however, vaccines are likely  
261 to contribute controlling SARS-CoV-2 infections in the short term.

262

## 263 **Acknowledgements**

264 We would like to thank Cambridge University Hospitals NHS Trust Occupational Health  
265 Department. We would also like to thank the NIHR Cambridge Clinical Research Facility and  
266 staff at CUH and. We would like to thank Eleanor Lim and Georgina Okecha. We thank Dr  
267 James Voss for the kind gift of HeLa cells stably expressing ACE2. RKG is supported by a  
268 Wellcome Trust Senior Fellowship in Clinical Science (WT108082AIA). LEM is supported by  
269 a Medical Research Council Career Development Award (MR/R008698/1). SAK is supported  
270 by the Bill and Melinda Gates Foundation via PANGAEA grant: OPP1175094. DAC is supported  
271 by a Wellcome Trust Clinical PhD Research Fellowship. KGCS is the recipient of a Wellcome  
272 Investigator Award (200871/Z/16/Z). This research was supported by the National Institute for  
273 Health Research (NIHR) Cambridge Biomedical Research Centre, the Cambridge Clinical  
274 Trials Unit (CCTU), and the NIHR BioResource. The views expressed are those of the authors  
275 and not necessarily those of the NIHR or the Department of Health and Social Care. JAGB is  
276 supported by the Medical Research Council (MC\_UP\_1201/16). IATM is funded by a  
277 SANTHE award.

278

279 **Author contributions**

280 Conceived study: D.C., RKG, DAC. Designed study and experiments: RKG, DAC, LEM, JB,  
281 MW, JT, LCG, GBM, RD, BG, NK, AE, M.P., D.V., L.P., A.D.M, J.B., D.C. Performed  
282 experiments: BM, DAC, RD, IATMF, LCG, GBM. Interpreted data: RKG, DAC, BM, RD,  
283 IATMF, LEM, JB, KGCS. A.D.M., J.B. and C.S.F. carried out pseudovirus neutralization  
284 assays. D.P. produced pseudoviruses. M.S.P., L.P., D.V. and D.C. designed the experiments.  
285 A.C.W., N.S. and S.J. expressed and purified the proteins. K.C., S.J. and E.C. sequenced and  
286 expressed antibodies. E.C. and K.C. performed mutagenesis for mutant expression plasmids.  
287 A.C.W. M.A.T., J.E.B., and S.B. performed binding assays. A.R., A.F.P and C.G contributed  
288 to donor's recruitment and sample collection related to mAbs isolation. H.W.V., G.S., A.L.,  
289 D.V., L.P. and D.C. analyzed the data and prepared the manuscript with input from all authors.

290 **Competing interests**

291 A.D.M., J.B., D.P., C.S.F., S.B., K.C., N.S., E.C., G.S., S.J., A.L., H.W.V., M.S.P., L.P. and  
292 D.C. are employees of Vir Biotechnology and may hold shares in Vir Biotechnology. H.W.V.  
293 is a founder of PierianDx and Casma Therapeutics. Neither company provided funding for this  
294 work or is performing related work. D.V. is a consultant for Vir Biotechnology Inc. The Veesler  
295 laboratory has received a sponsored research agreement from Vir Biotechnology Inc. The  
296 remaining authors declare that the research was conducted in the absence of any commercial  
297 or financial relationships that could be construed as a potential conflict of interest. RKG has  
298 received consulting fees from UMOVIS Lab, Gilead and ViiV.

299

300 **MATERIALS AND METHODS**

301 *Participant recruitment and ethics*

302 Participants who had received the first dose of vaccine and individuals with COVID-19 were  
303 consented into the Covid-19 cohort of the NIHR Bioresource. The study was approved by the  
304 East of England – Cambridge Central Research Ethics Committee (17/EE/0025).

305

306 *SARS-CoV-2 serology by multiplex particle-based flow cytometry (Luminex):*

307 Recombinant SARS-CoV-2 N, S and RBD were covalently coupled to distinct carboxylated  
308 bead sets (Luminex; Netherlands) to form a 3-plex and analyzed as previously described (Xiong  
309 et al. 2020). Specific binding was reported as mean fluorescence intensities (MFI).

310

311 *Recombinant expression of SARS-CoV-2-specific mAbs.*

312 Human mAbs were isolated from plasma cells or memory B cells of SARS-CoV-2 immune  
313 donors, as previously described<sup>40-42</sup>. Recombinant antibodies were expressed in ExpiCHO cells  
314 at 37°C and 8% CO<sub>2</sub>. Cells were transfected using ExpiFectamine. Transfected cells were  
315 supplemented 1 day after transfection with ExpiCHO Feed and ExpiFectamine CHO Enhancer.  
316 Cell culture supernatant was collected eight days after transfection and filtered through a 0.2  
317 µm filter. Recombinant antibodies were affinity purified on an ÄKTA xpress FPLC device  
318 using 5 mL HiTrap™ MabSelect™ Prisma columns followed by buffer exchange to Histidine  
319 buffer (20 mM Histidine, 8% sucrose, pH 6) using HiPrep 26/10 desalting columns

320

321 *Generation of S mutants*

322 Amino acid substitutions were introduced into the D614G pCDNA\_SARS-CoV-2\_S plasmid  
323 as previously described<sup>43</sup> using the QuikChange Lightning Site-Directed Mutagenesis kit,  
324 following the manufacturer's instructions (Agilent Technologies, Inc., Santa Clara, CA).  
325 Sequences were checked by Sanger sequencing.

326 Preparation of B.1.1.7 SARS-CoV-2 S glycoprotein-encoding-plasmid used to produce SARS-  
327 CoV-2-MLV based on overlap extension PCR. Briefly, a modification of the overlap extension  
328 PCR protocol<sup>44</sup> was used to introduce the nine mutations of the B.1.1.7 lineage in the SARS-  
329 CoV-2 S gene. In a first step, 9 DNA fragments with overlap sequences were amplified by  
330 PCR from a plasmid (pHCMV1, Genlantis) encoding the full-length SARS-CoV-2 S gene  
331 (BetaCoV/Wuhan-Hu-1/2019, accession number mn908947). The mutations (del-69/70, del-  
332 144, N501Y, A570D, D614G, P681H, S982A, T716I and D1118H) were introduced by  
333 amplification with primers with similar T<sub>m</sub>. Deletion of the C-terminal 21 amino acids was  
334 introduced to increase surface expression of the recombinant S<sup>45</sup>. Next, 3 contiguous  
335 overlapping fragments were fused by a first overlap PCR (step 2) using the utmost external  
336 primers of each set, resulting in 3 larger fragments with overlapping sequences. A final overlap  
337 PCR (step 3) was performed on the 3 large fragments using the utmost external primers to  
338 amplify the full-length S gene and the flanking sequences including the restriction  
339 sites KpnI and NotI. This fragment was digested and cloned into the expression plasmid  
340 pHCMV1. For all PCR reactions the Q5 Hot Start High fidelity DNA polymerase was used  
341 (New England Biolabs Inc.), according to the manufacturer's instructions and adapting the  
342 elongation time to the size of the amplicon. After each PCR step the amplified regions were  
343 separated on agarose gel and purified using Illustra GFX™ PCR DNA and Gel Band  
344 Purification Kit (Merck KGaA).

345

346 *Pseudotype virus preparation*

347 Viral vectors were prepared by transfection of 293T cells by using Fugene HD transfection  
348 reagent (Promega). 293T cells were transfected with a mixture of 11ul of Fugene HD, 1µg of  
349 pCDNAΔ19Spike-HA, 1ug of p8.91 HIV-1 gag-pol expression vector<sup>46,47</sup>, and 1.5µg of  
350 pCSFLW (expressing the firefly luciferase reporter gene with the HIV-1 packaging signal).  
351 Viral supernatant was collected at 48 and 72h after transfection, filtered through 0.45um filter  
352 and stored at -80°C. The 50% tissue culture infectious dose (TCID<sub>50</sub>) of SARS-CoV-2  
353 pseudovirus was determined using Steady-Glo Luciferase assay system (Promega).

354

355 *Serum/plasma pseudotype neutralization assay*

356 Spike pseudotype assays have been shown to have similar characteristics as neutralisation  
357 testing using fully infectious wild type SARS-CoV-2<sup>20</sup>. Virus neutralisation assays were  
358 performed on 293T cell transiently transfected with ACE2 and TMPRSS2 using SARS-CoV-2  
359 Spike pseudotyped virus expressing luciferase<sup>48</sup>. Pseudotyped virus was incubated with serial  
360 dilution of heat inactivated human serum samples or sera from vaccinees in duplicate for 1h at  
361 37°C. Virus and cell only controls were also included. Then, freshly trypsinized 293T  
362 ACE2/TMPRSS2 expressing cells were added to each well. Following 48h incubation in a 5%  
363 CO<sub>2</sub> environment at 37°C, luminescence was measured using the Steady-Glo Luciferase assay  
364 system (Promega).

365 *IFN $\gamma$  FLUOROSPOT assays*

366 Frozen PBMCs were rapidly thawed, and the freezing medium was diluted into 10ml of  
367 TexMACS media (Miltenyi Biotech), centrifuged and resuspended in 10ml of fresh media  
368 with 10U/ml DNase (Benzonase, Merck-Millipore via Sigma-Aldrich), PBMCs were  
369 incubated at 37°C for 1h, followed by centrifugation and resuspension in fresh media  
370 supplemented with 5% Human AB serum (Sigma Aldrich) before being counted. PBMCs  
371 were stained with 2ul of each antibody: anti-CD3-fluorescein isothiocyanate (FITC), clone  
372 UCHT1; anti-CD4-phycoerythrin (PE), clone RPA-T4; anti-CD8a-peridinin-chlorophyll  
373 protein - cyanine 5.5 (PerCP Cy5.5), clone RPA-8a (all BioLegend, London, UK),  
374 LIVE/DEAD Fixable Far Red Dead Cell Stain Kit (Thermo Fisher Scientific). PBMC  
375 phenotyping was performed on the BD Accuri C6 flow cytometer. Data were analysed with  
376 FlowJo v10 (Becton Dickinson, Wokingham, UK). 1.5 to 2.5 x 10<sup>5</sup> PBMCs were incubated

377 in pre-coated Fluorospot plates (Human IFN $\gamma$  FLUOROSPOT (Mabtech AB, Nacka Strand,  
378 Sweden)) in triplicate with peptide mixes specific for Spike, Nucleocapsid and Membrane  
379 proteins of SARS-CoV-2 (final peptide concentration 1  $\mu$ g/ml/peptide, Miltenyi Biotech) and  
380 an unstimulated and positive control mix (containing anti-CD3 (Mabtech AB),  
381 Staphylococcus Enterotoxin B (SEB), Phytohaemagglutinin (PHA) (all Sigma Aldrich)) at  
382 37°C in a humidified CO<sub>2</sub> atmosphere for 48 hours. The cells and medium were decanted  
383 from the plate and the assay developed following the manufacturer's instructions. Developed  
384 plates were read using an AID iSpot reader (Oxford Biosystems, Oxford, UK) and counted  
385 using AID EliSpot v7 software (Autoimmun Diagnostika GmbH, Strasberg, Germany). All  
386 data were then corrected for background cytokine production and expressed as SFU/Million  
387 PBMC or CD3 T cells.

388  
389 *MAbs pseudovirus neutralization assay*

390 MLV-based SARS-CoV-2 S-glycoprotein-pseudotyped viruses were prepared as previously  
391 described (Pinto et al., 2020). HEK293T/17cells were cotransfected with a WT or B.1.1.7  
392 SARS-CoV-2 Spike glycoprotein-encoding-plasmid, an MLV Gag-Pol packaging construct  
393 and the MLV transfer vector encoding a luciferase reporter using X-tremeGENE HP  
394 transfection reagent (Roche) according to the manufacturer's instructions. Cells were cultured  
395 for 72 h at 37°C with 5% CO<sub>2</sub> before harvesting the supernatant. VeroE6 stably expressing  
396 human TMPRSS2 were cultured in DMEM containing 10% FBS, 1% penicillin–streptomycin,  
397 8  $\mu$ g/mL puromycin and plated into 96-well plates for 16–24 h. Pseudovirus with serial dilution  
398 of mAbs was incubated for 1 h at 37°C and then added to the wells after washing 2 times with  
399 DMEM. After 2–3 h DMEM containing 20% FBS and 2% penicillin–streptomycin was added  
400 to the cells. Following 48-72 h of infection, Bio-Glo (Promega) was added to the cells and  
401 incubated in the dark for 15 min before reading luminescence with Synergy H1 microplate  
402 reader (BioTek). Measurements were done in duplicate and relative luciferase units were  
403 converted to percent neutralization and plotted with a non-linear regression model to determine  
404 IC<sub>50</sub> values using GraphPad PRISM software (version 9.0.0).

405  
406 *Antibody binding measurements using bio-layer interferometry (BLI)*

407 MAbs were diluted to 3  $\mu$ g/ml in kinetic buffer (PBS supplemented with 0.01% BSA) and  
408 immobilized on Protein A Biosensors (FortéBio). Antibody-coated biosensors were incubated  
409 for 3 min with a solution containing 5  $\mu$ g/ml of WT or N50Y SARS-CoV-2 RBD in kinetic  
410 buffer, followed by a 3-min dissociation step. Change in molecules bound to the biosensors



411 caused a shift in the interference pattern that was recorded in real time using an Octet RED96  
412 system (FortéBio). The binding response over time was used to calculate the area under the  
413 curve (AUC) using GraphPad PRISM software (version 9.0.0).

414

#### 415 *Production of SARS-CoV-2 and B.1.1.7 receptor binding domains and human ACE2*

416 The SARS-CoV-2 RBD (BEI NR-52422) construct was synthesized by GenScript into CMVR  
417 with an N-terminal mu-phosphatase signal peptide and a C-terminal octa-histidine tag  
418 (GHHHHHHHH) and an avi tag. The boundaries of the construct are N-<sub>328</sub>RFPN<sub>331</sub> and  
419 <sub>528</sub>KKST<sub>531</sub>-C<sup>49</sup>. The B.1.1.7 RBD was synthesized by GenScript into pCMVR with the same  
420 boundaries and construct details with a mutation at N501Y. These plasmids were transiently  
421 transfected into Expi293F cells using Expi293F expression medium (Life Technologies) at  
422 37°C 8% CO<sub>2</sub> rotating at 150 rpm. The cultures were transfected using PEI cultivated for  
423 5 days. Supernatants were clarified by centrifugation (10 min at 4000xg) prior to loading onto  
424 a nickel-NTA column (GE). Purified protein was biotinylated overnight using BirA (Avidity)  
425 prior to SEC into PBS. Human ACE2-Fc (residues 1-615 with a C-terminal thrombin cleavage  
426 site and human Fc tag) were synthesized by Twist. Clarified supernatants were affinity purified  
427 using a Protein A column (GE LifeSciences) directly neutralized and buffer exchanged. The  
428 Fc tag was removed by thrombin cleavage in a reaction mixture containing 3 mg of  
429 recombinant ACE2-FC ectodomain and 10 µg of thrombin in 20 mM Tris-HCl pH8.0, 150 mM  
430 NaCl and 2.5 mM CaCl<sub>2</sub>. The reaction mixture was incubated at 25°C overnight and re-loaded  
431 on a Protein A column to remove uncleaved protein and the Fc tag. The cleaved protein was  
432 further purified by gel filtration using a Superdex 200 column 10/300 GL (GE Life Sciences)  
433 equilibrated in PBS.

434

#### 435 *Protein affinity measurement using bio-layer interferometry*

436 Biotinylated RBD (either WT or N501Y) were immobilized at 5 ng/uL in undiluted 10X  
437 Kinetics Buffer (Pall) to SA sensors until a load level of 1.1nm, A dilution series of either  
438 monomeric ACE2 or Fab in undiluted kinetics buffer starting at 1000-50nM was used for 300-  
439 600 seconds to determine protein-protein affinity. The data were baseline subtracted and the  
440 plots fitted using the Pall FortéBio/Sartorius analysis software (version 12.0). Data were plotted  
441 in Prism.

442

443

444 **Table 1:** Vaccinee Participants and serum neutralisation data; ID50 (inhibitory dilution) is the  
 445 dilution required to achieve neutralisation of 50% infection by the virus. fold change (FC). NA:  
 446 not available.

ID	Age	Mean ID50 (SD) WT	Fold Change $\Delta 69/70$ 501Y 570D	Fold Change B.1.1.7 Spike mutations
1	60-65	34 (21)	0.435739	1.78
2	80-85	105 (62)	1.041735	2.18
3	40-45	93 (73)	0.32497	2.68
4	85-90	28 (15)	1.55961	-
5	25-30	27 (7)	0.386996	4.80
6	35-40	9 (0)	0.183133	4.46
7	80-85	27 (11)	0.383294	5.83
8	80-85	1 (0)	-	-
9	55-60	834 (658)	0.58253	2.88
10	85-90	1 (0)	-	-
11	80-85	2 (1)	-	-
12	80-85	3 (2)	-	-
13	80-85	4 (1)	-	-
14	85-90	41 (16)	0.468458	4.07025411
15	75-80	233 (104)	NA	6.12008534
16	80-85	1 (0)	-	-
17	80-85	1 (0)	-	-
18	85-90	723 (385)	0.674522	3.62182971
19	85-90	29 (7)	0.230936	5.41319667
20	80-85	63 (44)	0.538738	3.85473562
22	55-60	41 (17)	0.395114	5.27833669
25	60-65	52 (12)	0.808271	2.34132055
28	80-82	3449 (2489)	0.60931	3.17481581

447

448

449 **Table 2. Kinetic analysis of human ACE2 binding to SARS-CoV-2 B.1.1.7 and Wuhan-1**  
 450 **RBDs by biolayer interferometry.** Values reported represent the global fit to the data shown  
 451 in Extended Data Fig. 7.

		SARS-CoV-2 RBD WT	SARS-CoV-2 RBD B.1.1.7
<b>K<sub>D</sub> (nM)</b>		133	22
<b>k<sub>on</sub> (M<sup>-1</sup>.s<sup>-1</sup>)</b>	hACE2	1.3*10 <sup>5</sup>	1.4*10 <sup>5</sup>

$k_{\text{off}} \text{ (s}^{-1}\text{)}$		$1.8 \cdot 10^{-2}$	$3 \cdot 10^{-3}$
--	--	---------------------	-------------------

452

453

454

455

456

457

**Extended Data Table 1. Neutralization, V gene usage and other properties of tested mAbs.**

mAb	Domain (site)	VH usage (% id.)	Source (DSO)	IC50 WT (ng/ml)	IC50 B.1.1.7 (ng/ml)	ACE2 blocking	SARS-CoV	Escape residues	Ref.
4A8	NTD (i)	1-24	N/A	38	-	Neg.	-	S12P; C136Y; Y144del; H146Y; K147T; R246A	<sup>50</sup>
S2L26	NTD (i)	1-24 (97.2)	Hosp. (52)	70	-	Neg.	-	N/A	<sup>22</sup>
S2L50	NTD (i)	4-59 (95.4)	Hosp. (52)	264	50	Neg.	-	N/A	<sup>22</sup>
S2M28	NTD (i)	3-33 (97.6)	Hosp. (46)	295	12'207	Neg.	-	P9S/Q; S12P; C15F/R; L18P; Y28C; A123T; C136Y; G142D; Y144del; K147Q/T; R246G; P251L; G252C	<sup>22</sup>
S2X107	NTD (i)	4-38-2 (97)	Sympt. (75)	388	-	Neg.	-	N/A	<sup>22</sup>
S2X124	NTD (i)	3-30 (99)	Sympt. (75)	221	-	Neg.	-	N/A	<sup>22</sup>
S2X158	NTD (i)	1-24 (96.3)	Sympt. (75)	56	-	Neg.	-	N/A	<sup>22</sup>
S2X28	NTD (i)	3-30 (97.9)	Sympt. (48)	1'399	-	Neg.	-	P9S; S12P; C15W; L18P; C136G/Y; F140S; L141S; G142C/D; Y144C/N; K147T/Q/E; R158G; L244S; R246G	<sup>22</sup>
S2X303	NTD (i)	2-5 (95.9)	Sympt. (125)	69	-	Neg.	-	N/A	<sup>22</sup>
S2X333	NTD (i)	3-33 (96.5)	Sympt. (125)	66	-	Neg.	-	P9L; S12P; C15S/Y; L18P; C136G/Y; F140C; G142D; K147T	<sup>22</sup>
S2D106	RBD (I/RBM)	1-69 (97.2)	Hosp. (98)	27	20	Strong	-	N/A	<sup>8</sup>
S2D19	RBD (I/RBM)	4-31 (99.7)	Hosp. (49)	128	75'200	Moderate	-	N/A	<sup>8</sup>
S2D32	RBD (I/RBM)	3-49 (98.3)	Hosp. (49)	26	11	Strong	-	N/A	<sup>8</sup>
S2D65	RBD (I/RBM)	3-9 (96.9)	Hosp. (49)	24	12	Weak	-	N/A	<sup>8</sup>
S2D8	RBD (I/RBM)	3-23 (96.5)	Hosp. (49)	27	58'644	Strong	-	N/A	<sup>8</sup>
S2D97	RBD (I/RBM)	2-5 (96.9)	Hosp. (98)	20	17	Weak	-	N/A	<sup>8</sup>
S2E11	RBD (I/RBM)	4-61 (98.3)	Hosp. (51)	27	16	Weak	-	N/A	<sup>8</sup>
S2E12	RBD (I/RBM)	1-58 (97.6)	Hosp. (51)	27	31	Strong	-	G476S (3x)	<sup>8,51</sup>
S2E13	RBD (I/RBM)	1-18 (96.2)	Hosp. (51)	34	77	Strong	-	N/A	<sup>8</sup>
S2E16	RBD (I/RBM)	3-30 (98.3)	Hosp. (51)	36	38	Strong	-	N/A	<sup>8</sup>
S2E23	RBD (I/RBM)	3-64 (96.9)	Hosp. (51)	139	180	Strong	-	N/A	<sup>8</sup>
S2H14	RBD (I/RBM)	3-15 (100)	Sympt. (17)	460	64'463	Weak	-	N/A	<sup>8,52</sup>
S2H19	RBD (I/RBM)	3-15 (98.6)	Sympt. (45)	239	-	Weak	-	N/A	<sup>8</sup>
S2H58	RBD (I/RBM)	1-2 (97.9)	Sympt. (45)	27	14	Strong	-	N/A	<sup>8</sup>
S2H7	RBD (I/RBM)	3-66 (98.3)	Sympt. (17)	492	573	Weak	-	N/A	<sup>8</sup>
S2H70	RBD (I/RBM)	1-2 (99)	Sympt. (45)	147	65	Weak	-	N/A	<sup>8</sup>
S2H71	RBD (I/RBM)	2-5 (99)	Sympt. (45)	36	9	Moderate	-	N/A	<sup>8</sup>
S2M11	RBD (I/RBM)	1-2 (96.5)	Hosp. (46)	11	4	Weak	-	Y449N; L455F; E484K; E484Q; F490L; F490S; S494P	<sup>8,51</sup>

<b>S2N12</b>	RBD (I/RBM)	4-39 (97.6)	Hosp. (51)	76	40	Strong	-	N/A	<sup>8</sup>
<b>S2N22</b>	RBD (I/RBM)	3-23 (96.5)	Hosp. (51)	32	21	Strong	-	N/A	<sup>8</sup>
<b>S2N28</b>	RBD (I/RBM)	3-30 (97.2)	Hosp. (51)	72	21	Strong	-	N/A	<sup>8</sup>
<b>S2X128</b>	RBD (I/RBM)	1-69-2 (97.6)	Sympt. (75)	50	112	Strong	-	N/A	<sup>8</sup>
<b>S2X16</b>	RBD (I/RBM)	1-69 (97.6)	Sympt. (48)	45	103	Strong	-	N/A	<sup>8</sup>
<b>S2X192</b>	RBD (I/RBM)	1-69 (96.9)	Sympt. (75)	326	-	Weak	-	N/A	<sup>8</sup>
<b>S2X227</b>	RBD (I/RBM)	1-46 (97.9)	Sympt. (75)	26	14	Strong	-	N/A	
<b>S2X246</b>	RBD (I/RBM)	3-48 (96.2)	Sympt. (75)	35	30	Strong	-	N/A	
<b>S2X30</b>	RBD (I/RBM)	1-69 (97.9)	Sympt. (48)	32	53	Strong	-	N/A	<sup>8</sup>
<b>S2X324</b>	RBD (I/RBM)	2-5 (97.3)	Sympt. (125)	8	23	Strong	-	N/A	
<b>S2X58</b>	RBD (I/RBM)	1-46 (99)	Sympt. (48)	32	47	Strong	-	N/A	<sup>8</sup>
<b>S2H90</b>	RBD (II)	4-61 (96.6)	Sympt. (81)	77	32	Strong	+	N/A	<sup>8</sup>
<b>S2H94</b>	RBD (II)	3-23 (93.4)	Sympt. (81)	123	144	Strong	+	N/A	<sup>8</sup>
<b>S2H97</b>	RBD (V)	5-51 (98.3)	Sympt. (81)	513	248	Weak	+	N/A	
<b>S2K15</b>	RBD (II)	2-26 (99.3)	Sympt. (87)	361	235	0	+	N/A	
<b>S2K21</b>	RBD (II)	3-33 (96.2)	Sympt. (118)	201	189	0	+	N/A	
<b>S2K30</b>	RBD (II)	1-2 (97.2)	Sympt. (87)	185	134	0	+	N/A	
<b>S2K63v2</b>	RBD (II)	3-30-3 (95.6)	Sympt. (118)	144	215	0	+	N/A	
<b>S2L17</b>	RBD (?)	5-10-1 (98.3)	Hosp. (51)	313	127	Moderate	+	N/A	<sup>8</sup>
<b>S2L37</b>	RBD (II)	3-13 (98.3)	Hosp. (51)	14'370	824	Moderate	+	N/A	
<b>S2L49</b>	RBD (?)	3-30 (97.9)	Hosp. (51)	24	32	Neg.	+	N/A	<sup>8</sup>
<b>S2X259</b>	RBD (IIa)	1-69 (94.1)	Sympt. (75)	145	91	Moderate	+	N/A	
<b>S2X305</b>	RBD (?)	1-2 (95.1)	Sympt. (125)	34	21	Strong	-	N/A	
<b>S2X35</b>	RBD (IIa)	1-18 (98.6)	Sympt. (48)	140	143	Strong	+	N/A	<sup>52</sup>
<b>S2X450</b>	RBD (?)	2-26 (96.9)	Sympt. (271)	368	198	Strong	+	N/A	
<b>S2X475</b>	RBD (?)	3-21 (93.8)	Sympt. (271)	1'431	851	Strong	+	N/A	
<b>S2X607</b>	RBD (?)	3-66 (95.4)	Sympt. (271)	41	23	Strong	-	N/A	
<b>S2X608</b>	RBD (?)	1-33 (93.2)	Sympt. (271)	21	35	Strong	-	N/A	
<b>S2X609</b>	RBD (?)	1-69 (93.8)	Sympt. (271)	47	35	Strong	-	N/A	
<b>S2X613</b>	RBD (?)	1-2 (91.7)	Sympt. (271)	28	19	Strong	-	N/A	
<b>S2X615</b>	RBD (?)	3-11 (94.8)	Sympt. (271)	23	17	Strong	-	N/A	
<b>S2X619</b>	RBD (?)	1-69 (92.7)	Sympt. (271)	36	60	Strong	-	N/A	
<b>S2X620</b>	RBD (?)	3-53 (95.1)	Sympt. (271)	34	45	Strong	-	N/A	

id., identity. DSO, days after symptom onset. \* as described in Piccoli et al and McCallum et al. N/A, not available; -, not neutralizing

458

459

460

461 **References**

462

- 463 1 Zhou, P. *et al.* A pneumonia outbreak associated with a new coronavirus of probable  
464 bat origin. *Nature* **579**, 270-273, doi:10.1038/s41586-020-2012-7 (2020).
- 465 2 Davies, N. G. *et al.* Estimated transmissibility and severity of novel SARS-CoV-2  
466 Variant of Concern 202012/01 in England. *medRxiv*, 2020.2012.2024.20248822,  
467 doi:10.1101/2020.12.24.20248822 (2020).
- 468 3 Volz, E. *et al.* Transmission of SARS-CoV-2 Lineage B.1.1.7 in England: Insights from  
469 linking epidemiological and genetic data. *medRxiv*, 2020.2012.2030.20249034,  
470 doi:10.1101/2020.12.30.20249034 (2021).
- 471 4 Korber, B. *et al.* Tracking Changes in SARS-CoV-2 Spike: Evidence that D614G  
472 Increases Infectivity of the COVID-19 Virus. *Cell* **182**, 812-827 e819,  
473 doi:10.1016/j.cell.2020.06.043 (2020).
- 474 5 Yurkovetskiy, L. *et al.* Structural and Functional Analysis of the D614G SARS-CoV-2  
475 Spike Protein Variant. *Cell* **183**, 739-751 e738, doi:10.1016/j.cell.2020.09.032 (2020).
- 476 6 Martinot, M. *et al.* Remdesivir failure with SARS-CoV-2 RNA-dependent RNA-  
477 polymerase mutation in a B-cell immunodeficient patient with protracted Covid-19.  
478 *Clin Infect Dis*, doi:10.1093/cid/ciaa1474 (2020).
- 479 7 Kemp, S. *et al.* Neutralising antibodies in Spike mediated SARS-CoV-2 adaptation.  
480 *medRxiv*, 2020.2012.2005.20241927, doi:10.1101/2020.12.05.20241927 (2020).
- 481 8 Thomson, E. C. *et al.* The circulating SARS-CoV-2 spike variant N439K maintains  
482 fitness while evading antibody-mediated immunity. *bioRxiv*, 1-49,  
483 doi:papers3://publication/doi/10.1101/2020.11.04.355842 (2020).
- 484 9 Baden, L. R. *et al.* Efficacy and Safety of the mRNA-1273 SARS-CoV-2 Vaccine. *N Engl*  
485 *J Med*, doi:10.1056/NEJMoa2035389 (2020).
- 486 10 Polack, F. P. *et al.* Safety and Efficacy of the BNT162b2 mRNA Covid-19 Vaccine. *N*  
487 *Engl J Med* **383**, 2603-2615, doi:10.1056/NEJMoa2034577 (2020).
- 488 11 Voysey, M. *et al.* Safety and efficacy of the ChAdOx1 nCoV-19 vaccine (AZD1222)  
489 against SARS-CoV-2: an interim analysis of four randomised controlled trials in Brazil,  
490 South Africa, and the UK. *Lancet* **397**, 99-111, doi:10.1016/S0140-6736(20)32661-1  
491 (2021).
- 492 12 Mulligan, M. J. *et al.* Phase I/II study of COVID-19 RNA vaccine BNT162b1 in adults.  
493 *Nature* **586**, 589-593, doi:10.1038/s41586-020-2639-4 (2020).
- 494 13 Corbett, K. S. *et al.* SARS-CoV-2 mRNA Vaccine Development Enabled by Prototype  
495 Pathogen Preparedness. *bioRxiv*, 2020.2006.2011.145920,  
496 doi:10.1101/2020.06.11.145920 (2020).
- 497 14 Folegatti, P. M. *et al.* Safety and immunogenicity of the ChAdOx1 nCoV-19 vaccine  
498 against SARS-CoV-2: a preliminary report of a phase 1/2, single-blind, randomised  
499 controlled trial. *Lancet* **396**, 467-478, doi:10.1016/S0140-6736(20)31604-4 (2020).
- 500 15 Kemp, S. A. *et al.* Recurrent emergence and transmission of a SARS-CoV-2 Spike  
501 deletion  $\Delta$ H69/V70. *bioRxiv*, 2020.2012.2014.422555,  
502 doi:10.1101/2020.12.14.422555 (2020).
- 503 16 Tegally, H. *et al.* Emergence and rapid spread of a new severe acute respiratory  
504 syndrome-related coronavirus 2 (SARS-CoV-2) lineage with multiple spike mutations  
505 in South Africa. *medRxiv*, 2020.2012.2021.20248640,  
506 doi:10.1101/2020.12.21.20248640 (2020).

- 507 17 Faria, N. R. *et al.* Genomic characterisation of an emergent SARS-CoV-2 lineage in  
508 Manaus: preliminary findings, <[https://virological.org/t/genomic-characterisation-](https://virological.org/t/genomic-characterisation-of-an-emergent-sars-cov-2-lineage-in-manaus-preliminary-findings/586)  
509 [of-an-emergent-sars-cov-2-lineage-in-manaus-preliminary-findings/586](https://virological.org/t/genomic-characterisation-of-an-emergent-sars-cov-2-lineage-in-manaus-preliminary-findings/586)> (2021).
- 510 18 Jackson, L. A. *et al.* An mRNA Vaccine against SARS-CoV-2 - Preliminary Report. *N*  
511 *Engl J Med* **383**, 1920-1931, doi:10.1056/NEJMoa2022483 (2020).
- 512 19 Walsh, E. E. *et al.* Safety and Immunogenicity of Two RNA-Based Covid-19 Vaccine  
513 Candidates. *New England Journal of Medicine* **383**, 2439-2450,  
514 doi:10.1056/NEJMoa2027906 (2020).
- 515 20 Schmidt, F. *et al.* Measuring SARS-CoV-2 neutralizing antibody activity using  
516 pseudotyped and chimeric viruses. 2020.2006.2008.140871,  
517 doi:10.1101/2020.06.08.140871 %J bioRxiv (2020).
- 518 21 Brouwer, P. J. M. *et al.* Potent neutralizing antibodies from COVID-19 patients define  
519 multiple targets of vulnerability. *Science* **369**, 643-650, doi:10.1126/science.abc5902  
520 (2020).
- 521 22 McCallum, M. *et al.* N-terminal domain antigenic mapping reveals a site of  
522 vulnerability for SARS-CoV-2. *bioRxiv*, doi:10.1101/2021.01.14.426475 (2021).
- 523 23 Walls, A. C. *et al.* Structure, Function, and Antigenicity of the SARS- CoV-2 Spike  
524 Glycoprotein. *Cell* **181**, 281-292.e286,  
525 doi:papers3://publication/doi/10.1016/j.cell.2020.02.058 (2020).
- 526 24 Guan, Y. *et al.* Isolation and characterization of viruses related to the SARS  
527 coronavirus from animals in southern China. *Science* **302**, 276-278,  
528 doi:10.1126/science.1087139 (2003).
- 529 25 Li, W. *et al.* Efficient replication of severe acute respiratory syndrome coronavirus in  
530 mouse cells is limited by murine angiotensin-converting enzyme 2. *J Virol* **78**, 11429-  
531 11433, doi:10.1128/JVI.78.20.11429-11433.2004 (2004).
- 532 26 Li, W. *et al.* Receptor and viral determinants of SARS-coronavirus adaptation to  
533 human ACE2. *EMBO J* **24**, 1634-1643, doi:10.1038/sj.emboj.7600640 (2005).
- 534 27 Starr, T. N. *et al.* Deep Mutational Scanning of SARS-CoV-2 Receptor Binding Domain  
535 Reveals Constraints on Folding and ACE2 Binding. *Cell* **182**, 1295-1310 e1220,  
536 doi:10.1016/j.cell.2020.08.012 (2020).
- 537 28 Verschoor, C. P. *et al.* Microneutralization assay titres correlate with protection  
538 against seasonal influenza H1N1 and H3N2 in children. *PloS one* **10**, e0131531,  
539 doi:10.1371/journal.pone.0131531 (2015).
- 540 29 Kulkarni, P. S., Hurwitz, J. L., Simoes, E. A. F. & Piedra, P. A. Establishing Correlates of  
541 Protection for Vaccine Development: Considerations for the Respiratory Syncytial  
542 Virus Vaccine Field. *Viral Immunol* **31**, 195-203, doi:10.1089/vim.2017.0147 (2018).
- 543 30 Goddard, N. L., Cooke, M. C., Gupta, R. K. & Nguyen-Van-Tam, J. S. Timing of  
544 monoclonal antibody for seasonal RSV prophylaxis in the United Kingdom. *Epidemiol*  
545 *Infect* **135**, 159-162, doi:10.1017/S0950268806006601 (2007).
- 546 31 Mercado, N. B. *et al.* Single-shot Ad26 vaccine protects against SARS-CoV-2 in rhesus  
547 macaques. *Nature* **586**, 583-588, doi:10.1038/s41586-020-2607-z (2020).
- 548 32 McMahan, K. *et al.* Correlates of protection against SARS-CoV-2 in rhesus macaques.  
549 *Nature*, doi:10.1038/s41586-020-03041-6 (2020).
- 550 33 Wang, Z. *et al.* mRNA vaccine-elicited antibodies to SARS-CoV-2 and circulating  
551 variants. *bioRxiv*, doi:10.1101/2021.01.15.426911 (2021).

552 34 Wu, K. *et al.* mRNA-1273 vaccine induces neutralizing antibodies against spike  
553 mutants from global SARS-CoV-2 variants. *bioRxiv*, doi:10.1101/2021.01.25.427948  
554 (2021).

555 35 Soh, W. T. *et al.* The N-terminal domain of spike glycoprotein mediates SARS-CoV-2  
556 infection by associating with L-SIGN and DC-SIGN. 1-30,  
557 doi:papers3://publication/doi/10.1101/2020.11.05.369264 (2020).

558 36 Wibmer, C. K. *et al.* SARS-CoV-2 501Y.V2 escapes neutralization by South African  
559 COVID-19 donor plasma. *bioRxiv*, doi:10.1101/2021.01.18.427166 (2021).

560 37 Greaney, A. J. *et al.* Comprehensive mapping of mutations to the SARS-CoV-2  
561 receptor-binding domain that affect recognition by polyclonal human serum  
562 antibodies. *bioRxiv*, 2020.2012.2031.425021, doi:10.1101/2020.12.31.425021  
563 (2021).

564 38 Greaney, A. J. *et al.* Complete mapping of mutations to the SARS-CoV-2 spike  
565 receptor-binding domain that escape antibody recognition. *Cell Host & Microbe*  
566 (2020).

567 39 Weisblum, Y. *et al.* Escape from neutralizing antibodies by SARS-CoV-2 spike protein  
568 variants. *Elife* **9**, e61312, doi:10.7554/eLife.61312 (2020).

569 40 Corti, D. *et al.* A neutralizing antibody selected from plasma cells that binds to group  
570 1 and group 2 influenza A hemagglutinins. *Science* **333**, 850-856,  
571 doi:10.1126/science.1205669 (2011).

572 41 Pinto, D. *et al.* Cross-neutralization of SARS-CoV-2 by a human monoclonal SARS-CoV  
573 antibody. *Nature* **583**, 290-295, doi:10.1038/s41586-020-2349-y (2020).

574 42 Tortorici, M. A. *et al.* Ultrapotent human antibodies protect against SARS-CoV-2  
575 challenge via multiple mechanisms. *Science*, doi:10.1126/science.abe3354 (2020).

576 43 Gregson, J. *et al.* HIV-1 viral load is elevated in individuals with reverse transcriptase  
577 mutation M184V/I during virological failure of first line antiretroviral therapy and is  
578 associated with compensatory mutation L74I. *Journal of Infectious Diseases* (2019).

579 44 Forloni, M., Liu, A. Y. & Wajapeyee, N. Creating Insertions or Deletions Using Overlap  
580 Extension Polymerase Chain Reaction (PCR) Mutagenesis. *Cold Spring Harb Protoc*  
581 **2018**, doi:10.1101/pdb.prot097758 (2018).

582 45 Case, J. B. *et al.* Neutralizing Antibody and Soluble ACE2 Inhibition of a Replication-  
583 Competent VSV-SARS-CoV-2 and a Clinical Isolate of SARS-CoV-2. *Cell Host Microbe*  
584 **28**, 475-485 e475, doi:10.1016/j.chom.2020.06.021 (2020).

585 46 Naldini, L., Blomer, U., Gage, F. H., Trono, D. & Verma, I. M. Efficient transfer,  
586 integration, and sustained long-term expression of the transgene in adult rat brains  
587 injected with a lentiviral vector. *Proc Natl Acad Sci U S A* **93**, 11382-11388,  
588 doi:10.1073/pnas.93.21.11382 (1996).

589 47 Gupta, R. K. *et al.* Full length HIV-1 gag determines protease inhibitor susceptibility  
590 within in vitro assays. *AIDS* **24**, 1651 (2010).

591 48 Mlcochova, P. *et al.* Combined point of care nucleic acid and antibody testing for  
592 SARS-CoV-2 following emergence of D614G Spike Variant. *Cell Rep Med*, 100099,  
593 doi:10.1016/j.xcrm.2020.100099 (2020).

594 49 Walls, A. C. *et al.* Elicitation of Potent Neutralizing Antibody Responses by Designed  
595 Protein Nanoparticle Vaccines for SARS-CoV-2. *Cell* **183**, 1367-1382 e1317,  
596 doi:10.1016/j.cell.2020.10.043 (2020).



597 50 Chi, X. *et al.* A neutralizing human antibody binds to the N-terminal domain of the  
598 Spike protein of SARS-CoV-2. *Science*, eabc6952-6913,  
599 doi:papers3://publication/doi/10.1126/science.abc6952 (2020).  
600 51 Tortorici, M. A. *et al.* Ultrapotent human antibodies protect against SARS-CoV-2  
601 challenge via multiple mechanisms. *Science* **4**, eabe3354-3316,  
602 doi:papers3://publication/doi/10.1126/science.abe3354 (2020).  
603 52 Piccoli, L. *et al.* Mapping neutralizing and immunodominant sites on the SARS-CoV-2  
604 spike receptor-binding domain by structure-guided high-resolution serology. *Cell*, 1-  
605 55, doi:papers3://publication/doi/10.1016/j.cell.2020.09.037 (2020).  
606

# Figures

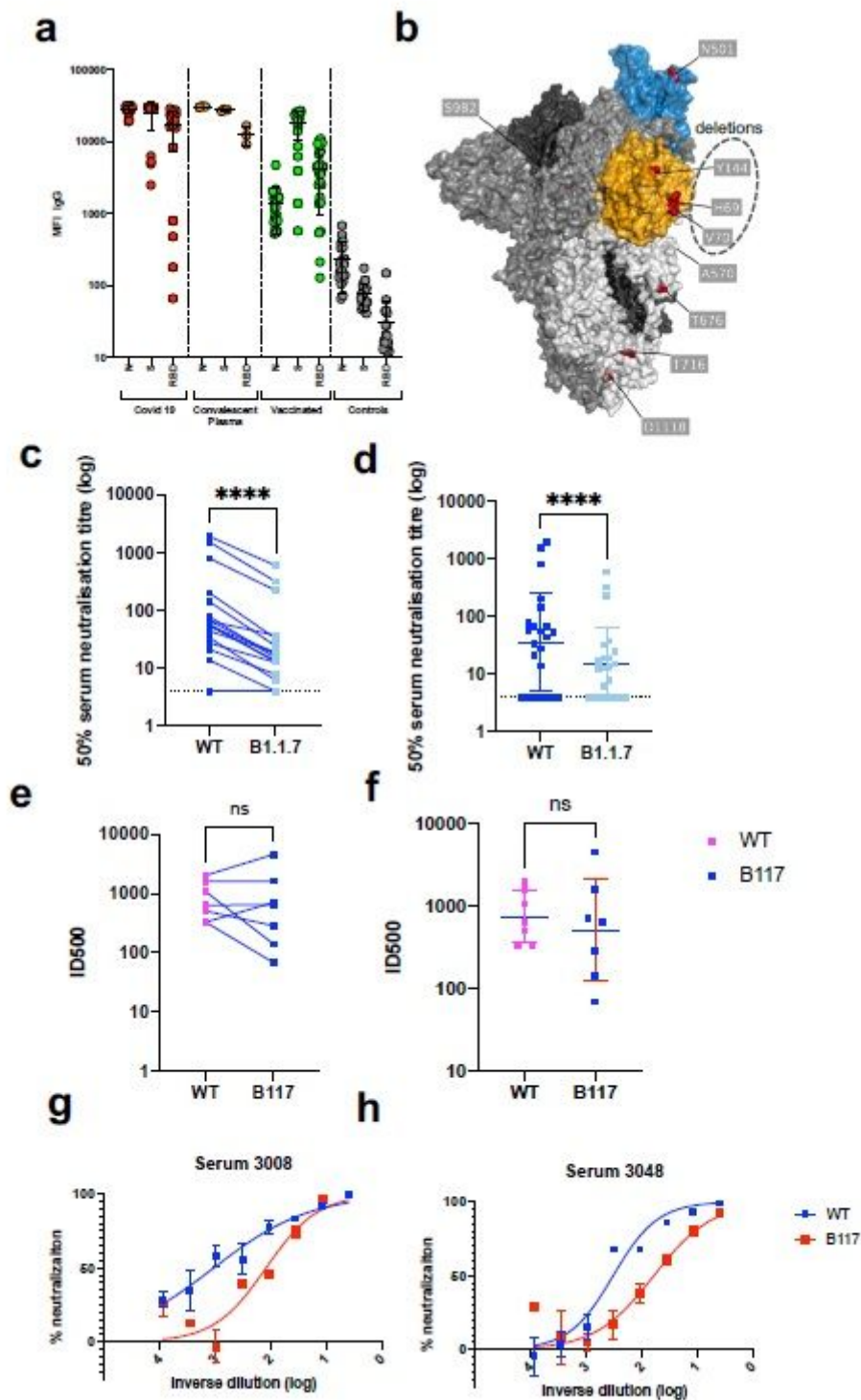


**Figure 1**

Neutralisation by sera against wild type and B.1.1.7 Spike mutant SARS-CoV-2 pseudotyped viruses. a, Serum IgG responses against N protein, Spike and the Spike Receptor Binding Domain (RBD) from 23 vaccinated participants (green), 20 recovered COVID-19 cases (red), 3 convalescent plasma units and 20

healthy controls (grey) as measured by a flow cytometry based Luminex assay. MFI, mean fluorescence intensity. b, Spike in open conformation with a single erect RBD (PDB: 6ZGG) in trimer axis vertical view with the locations of mutated residues highlighted in red spheres and labelled on the monomer with erect RBD. Vaccine (c-d) and convalescent sera (e-f) against WT and B.1.1.7 Spike mutant with N501Y, A570D, H69/V70, I144/145, P681H, T716I, S982A and D1118H. g-h, neutralisation curves for serum from two convalescent individuals with reduced susceptibility to B.1.1.7 Spike mutant, means of technical replicates are plotted with error bars representing standard error of mean. Data are representative of 2 independent experiments.

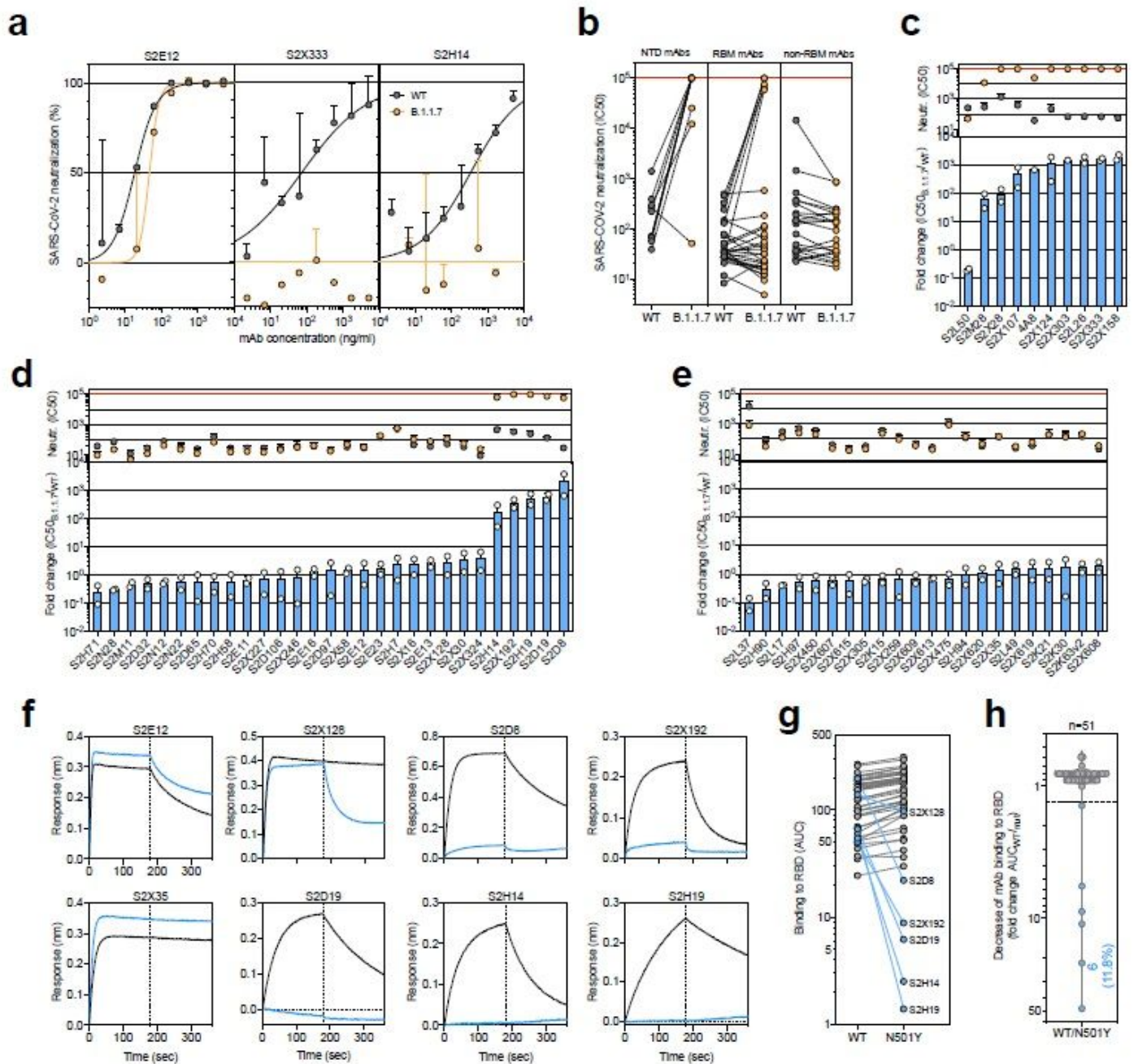
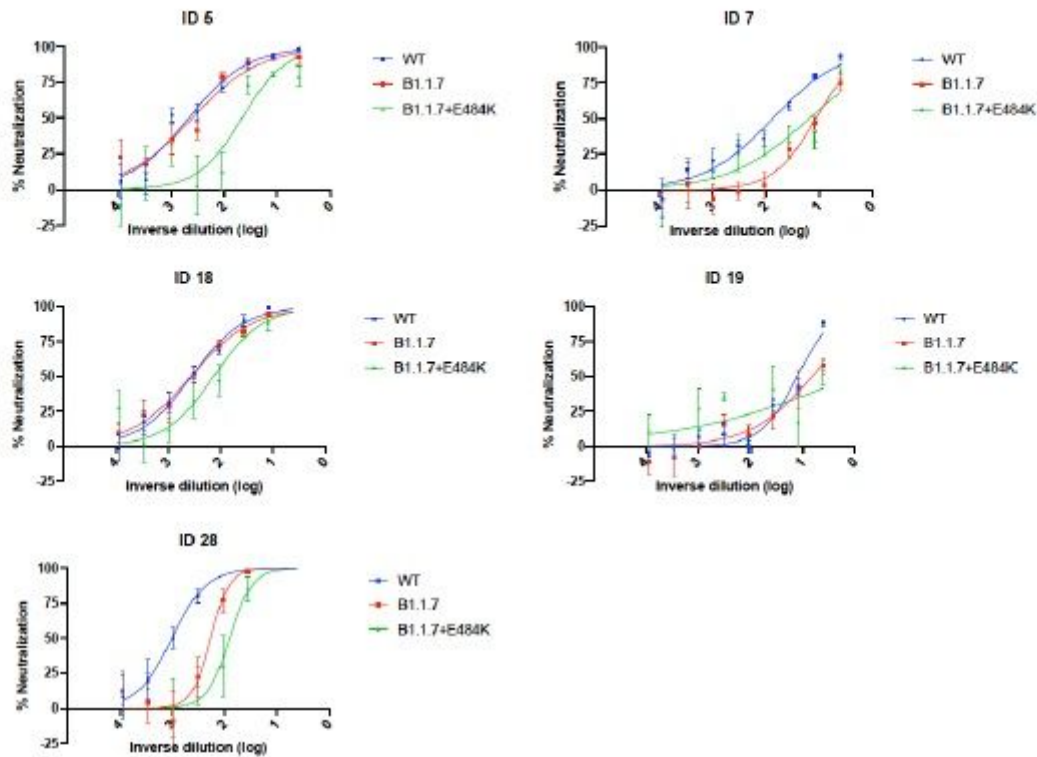
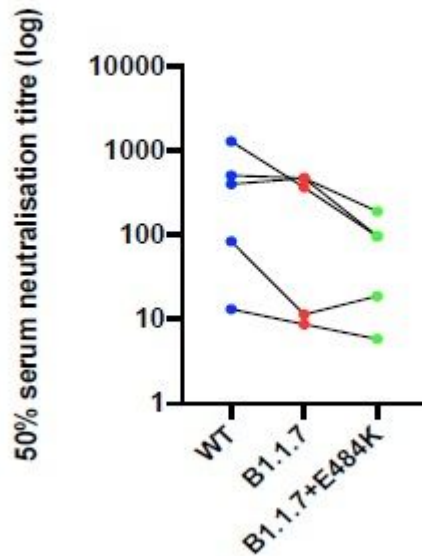
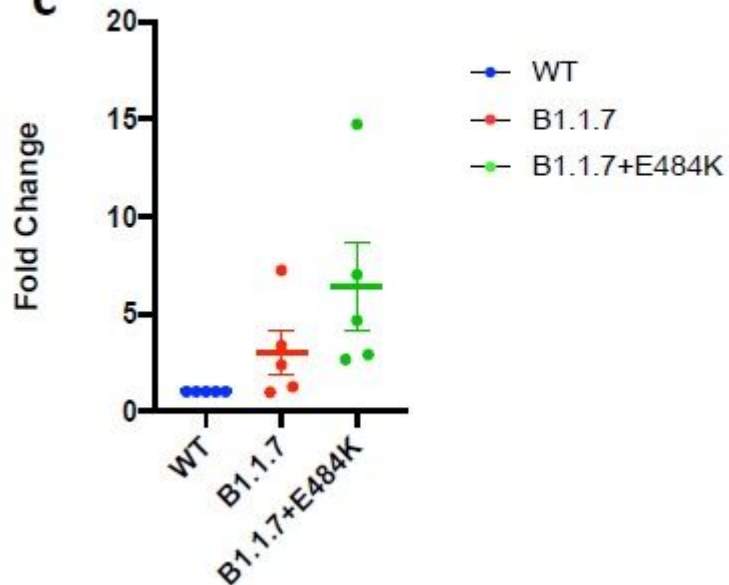


Figure 2

Neutralisation and binding by a panel of NTD- and RBD-specific mAbs against WT and B.1.1.7 SARS-CoV-2 viruses. a, Neutralisation of WT (black) and B.1.1.7 (orange) Spike pseudotyped SARS-CoV-2-MLV by 3 selected mAbs (S2E12, S2X333 and S2H14) from one representative experiment. Shown is the mean  $\pm$  s.d. of 2 technical replicates. b, Neutralisation of WT and B.1.1.7 SARS-CoV-2-MLV by 61 mAbs targeting NTD (n=10), RBM (n=29) and non-RBM sites in the RBD (n=22). Shown are the mean IC50 values (ng/ml) of n=2 independent experiments. c-e, Neutralisation shown as mean IC50 values (upper panel) and mean fold change of B.1.1.7 relative to WT (lower panel) of NTD (c), RBM (d) and non-RBM (e) mAbs. Lower panel shows IC50 values from 2 independent experiments. f-h, Kinetics of binding of mAbs to WT (black) and N501Y (blue) RBD as measured by bio-layer interferometry (BLI). Shown in (f) are the 6 RBM-targeting mAbs with reduced binding to N501Y RBD and 2 representative mAbs (RBM-targeting S2E12 and non-RBMtargeting S2X35). Area under the curve (AUC) (g) and AUC fold change (h) of 51 mAbs tested against WT and N501Y RBD. mAbs with a >1.3 AUC fold change shown in blue.

**a****b****c****Figure 3**

Neutralisation potency of vaccine sera against pseudovirus virus bearing Spike mutations in the B1.1.7 lineage with and without E484K in the receptor binding domain (all In Spike D614G background). a, Neutralisation curves for five vaccinated individuals. b. Indicated is 50% neutralisation titre for each virus and in c. data are expressed as fold change relative to WT. Data points represent means of two independent experiments.

## Supplementary Files

This is a list of supplementary files associated with this preprint. Click to download.

- [SupplementalFigures.pdf](#)